

Quasi-bound states in the continuum: a dynamical coupled-channel calculation of axial-vector charmed mesons

Susana Coito* and George Rupp†

*Centro de Física das Interações Fundamentais, Instituto Superior Técnico,
Technical University of Lisbon, P-1049-001 Lisboa, Portugal*

Eef van Beveren‡

*Centro de Física Computacional, Departamento de Física,
Universidade de Coimbra, P-3004-516 Coimbra, Portugal*

(Dated: October 27, 2011)

Masses and widths of the axial-vector charmed mesons $D_1(2420)$, $D_1(2430)$, $D_{s1}(2536)$, and $D_{s1}(2460)$ are calculated nonperturbatively in the Resonance-Spectrum-Expansion model, by coupling various open and closed meson-meson channels to the bare $J^P = 1^+ c\bar{q}$ ($q = u, d$) and $c\bar{s}$ states. The coupling to two-meson channels dynamically mixes and lifts the mass degeneracy of the spectroscopic 3P_1 and 1P_1 states, as an alternative to the usual spin-orbit splitting. Of the two resulting S -matrix poles in either case, one stays very close to the energy of the bare state, as a quasi-bound state in the continuum, whereas the other shifts considerably. This is in agreement with the experimental observation that the $D_1(2420)$ and $D_{s1}(2536)$ have much smaller widths than one would naively expect. The whole pattern of masses and widths of the axial-vector charmed mesons can thus be quite well reproduced with only two free parameters, one of which being already strongly constrained by previous model calculations. Finally, predictions for pole positions of radially excited axial-vector charmed mesons are presented.

PACS numbers: 14.40.Lb, 13.25.Ft, 11.80.Gw, 11.55.Ds, 12.40.Yx,

I. INTRODUCTION

The axial-vector (AV) charmed mesons $D_1(2420)$ and $D_{s1}(2536)$ [1] have the puzzling feature that their decay widths are much smaller than one would expect on the basis of their principal S -wave decay modes. Namely, the $D_1(2420)$ decays to $D^*\pi$ (possibly also in a D wave), with a phase space of more than 270 MeV, but has a total width of only 20–25 MeV [1]. On the other hand, the $D_{s1}(2536)$ decays to D^*K in S and D wave with a phase space of about 30 MeV, resulting in an unknown tiny width < 2.3 MeV, limited by the experimental resolution [1]. The discovery of the missing two AV charmed mesons, namely the very narrow $D_{s1}(2460)$ and the very broad $D_1(2430)$, first observed by CLEO [2] and Belle [3], respectively, completed an even more confusing picture. While the tiny width of the $D_{s1}(2460)$ can be easily understood, since this meson lies underneath its lowest Okubo-Zweig-Iizuka-allowed (OZIA) and isospin-conserving decay threshold, the huge $D_1(2430)$ width, in $D^*\pi$, is in sharp contrast with that of the $D_1(2420)$. Moreover, the $D_{s1}(2460)$ lies 76 MeV below the $D_{s1}(2536)$, whereas the $D_1(2420)$ and $D_1(2430)$ are almost degenerate in mass, if one takes the central value of the latter resonance.

Quark potential models, with standard spin-orbit split-

tings, fail dramatically in reproducing this pattern of masses. For instance, in the relativized quark model [4] the $c\bar{s}$ state that is mainly 3P_1 comes out at 2.57 GeV, assuming the already then well-established $D_{s1}(2536)$ to be mostly 1P_1 , though with a very large mixing between 3P_1 and 1P_1 . Reference [4] similarly predicted a too high mass for the dominantly 3P_1 state in the $c\bar{q}$ ($q = u, d$) sector, viz. 2.49 GeV. In the chiral quark model for heavy-light systems of Ref. [5], the result for the mainly 3P_1 $c\bar{q}$ state is also 2.49 GeV, while the discrepancy is even worse in the $c\bar{s}$ sector, with a prediction of 2.605 GeV for the mostly 3P_1 state, now with a small mixing in both sectors.

More recently and after the discovery of the $D_{s1}(2460)$ (and $D_1(2430)$), chiral Lagrangians for heavy-light systems (see e.g. Refs. [6–9]) have been employed in order to understand the masses of the AV charmed mesons, in particular the mass splittings with respect to the vector (V) mesons with charm D_s^* and D^* , respectively. Reference [7] analyzed in detail the curious experimental [1] observation that the AV-V mass difference is considerably larger in the charm-nonstrange sector than in the charm-strange one, which is not predicted by typical quark potential models [4, 5]. The same discrepancy applies to the scalar-pseudoscalar mass difference in either sector [1, 7]. In Ref. [7], the problem was tackled by calculating chiral loop corrections, but the result turned out to be exactly the opposite of what is needed to remove or alleviate the discrepancy.

An alternative approach to the AV charmed mesons is by trying to generate them as dynamical resonances in chiral unitary theory [10]. Indeed, in the latter paper, describing AV mesons in other flavor sectors as

*Electronic address: susana.coito@ist.utl.pt

†Electronic address: george@ist.utl.pt

‡Electronic address: eef@teor.fis.uc.pt

well, several charmed resonances were predicted, including the $D_1(2420)$, $D_1(2430)$, $D_{s1}(2536)$, and $D_{s1}(2460)$, with reasonable results, though the $c\bar{q}$ states came out about 100 MeV off. However, dynamical generation of mesonic resonances, including the ones that are commonly thought to be of a normal quark-antiquark type, may give rise to interpretational difficulties, besides predicting several genuinely exotic and so far unobserved states [10]. Dynamically generated AV charmed as well as bottom mesons can be found in Ref. [11], too.

Finally, in Ref. [12] a coupled-channel calculation of positive-parity $c\bar{s}$ and $b\bar{s}$ was carried out in a chiral quark model, similar to our approach in its philosophy, and with results for the $D_{s1}(2536)$ and $D_{s1}(2460)$ close to the present ones (also see below).

II. RESONANCE-SPECTRUM EXPANSION

In the present paper, we employ the Resonance-Spectrum Expansion (RSE) to describe the AV charmed mesons. The RSE model has been developed for meson-meson (MM) scattering in non-exotic channels, whereby the intermediate state is described via an infinite tower of s -channel $q\bar{q}$ states [13]. For the spectrum of the latter, in principle any confinement potential can be employed, but in practical applications, a harmonic oscillator (HO) with constant frequency has been used, with excellent results [13]. Recent applications of the RSE concern the $\phi(2170)$ [14] and $X(3872)$ [15] resonances.

In order to account for the two possible spectroscopic channels 3P_1 and 1P_1 contributing to a $J^P = 1^+$ state with undefined C -parity, we couple both $q\bar{q}$ channels to the most important meson-meson channels. The resulting fully off-energy-shell RSE T matrix reads [13–15]

$$T_{ij}^{(L_i, L_j)}(p_i, p'_j; E) = -2\lambda^2 \sqrt{\mu_i p_i r_0} j_{L_i}^i(p_i r_0) \times \sum_{m=1}^N \mathcal{R}_{im} \{[\mathbb{1} - \Omega \mathcal{R}]^{-1}\}_{mj} j_{L_j}^j(p'_j r_0) \sqrt{\mu_j p'_j r_0}, \quad (1)$$

with the diagonal loop function

$$\Omega_{ij}(k_j) = -2i\lambda^2 \mu_j k_j r_0 j_{L_j}^j(k_j r_0) h_{L_j}^{(1)j}(k_j r_0) \delta_{ij}, \quad (2)$$

and the RSE propagator

$$\mathcal{R}_{ij}(E) = \sum_{S=0,1} \sum_{n=0}^{\infty} \frac{g_{(S,n)}^i g_{(S,n)}^j}{E - E_n^{(S)}}. \quad (3)$$

Here, λ is an overall coupling, r_0 is the average distance for decay via 3P_0 quark-pair creation, $E_n^{(S)}$ is the discrete energy of the n -th recurrence in the $q\bar{q}$ channel with spin S , $g_{(S,n)}^i$ is the corresponding coupling to the i -th MM channel, μ_i the reduced mass for this channel, p_i the off-shell relative momentum, L_i the orbital angular momentum, and $j_{L_i}^i$ and $h_{L_j}^{(1)j}(k_j r_0)$ the spherical

Bessel and Hankel functions of the first kind, respectively. Note that μ_i , p_i , and the on-energy-shell relative momentum k_i are defined relativistically. Also notice that the infinite sum over the higher recurrences converges very fast, so that it can be truncated after 20 terms in practical calculations. The S matrix is finally given by $S_{ij}^{(L_i, L_j)}(E) = 1 + 2iT_{ij}^{(L_i, L_j)}(k_i, k_j; E)$.

III. OZI-ALLOWED CHANNELS FOR AV CHARMED MESONS

Now we describe the physical AV charmed resonances by coupling bare 3P_1 and 1P_1 $c\bar{q}$, $c\bar{s}$ channels to all OZI-allowed ground-state pseudoscalar-vector (PV) and vector-vector (VV) channels. It is true that there are also relevant pseudoscalar-scalar (PS) channels (in P -wave), most notably $Df_0(600)$ and $D_0^*(2400)\pi$ [1] in the AV $c\bar{q}$ case, and $DK_0^*(800)$ for $c\bar{s}$. These will contribute to the observed [1] $D\pi\pi$ and $D\pi K$ decay modes, respectively. Now, we have recently developed [15] an algebraic procedure to deal with resonances in asymptotic states whilst preserving unitarity. However, the huge widths of the $D_0^*(2400)$, $f_0(600)$, and $K_0^*(800)$ resonances may lead to fine sensitivities that will tend to obscure the point we want to make, apart from the fact that there will also be nonresonant contributions to the $D\pi\pi$ and $D\pi K$ final

TABLE I: Included meson-meson channels for $D_1(2420)$ and $D_1(2430)$, with ground-state couplings squared [16], orbital angular momenta, and thresholds in MeV. For η and η' , a pseudoscalar mixing angle of 37.3° [14] is used.

Channel	$(\tilde{g}_{(S=1, n=0)}^i)^2$	$(\tilde{g}_{(S=0, n=0)}^j)^2$	L	Threshold
$D^*\pi$	0.02778	0.01389	0	2146
$D^*\pi$	0.03472	0.06944	2	2146
$D^*\eta$	0.00524	0.00262	0	2556
$D^*\eta$	0.00655	0.01310	2	2556
D_s^*K	0.01852	0.00926	0	2608
D_s^*K	0.02315	0.04630	2	2608
$D\rho$	0.02778	0.01389	0	2643
$D\rho$	0.03472	0.06944	2	2643
$D\omega$	0.00926	0.00463	0	2650
$D\omega$	0.01157	0.02315	2	2650
$D^*\rho$	0	0.01389	0	2784
$D^*\rho$	0.01042	0.06944	2	2784
$D^*\omega$	0	0.00463	0	2791
$D^*\omega$	0.03472	0.02315	2	2791
$D_s K^*$	0.01852	0.00926	0	2862
$D_s K^*$	0.02315	0.04630	2	2862
$D^*\eta'$	0.00402	0.00201	0	2996
$D^*\eta'$	0.00502	0.01004	2	2996
$D_s^* K^*$	0	0.00926	0	3006
$D_s^* K^*$	0.06944	0.04630	2	3006

TABLE II: As Table I, but now for $D_{s1}(2536)$ and $D_{s1}(2460)$.

Channel	$(\tilde{g}_{(S=1,n=0)}^i)^2$	$(\tilde{g}_{(S=0,n=0)}^i)^2$	L	Threshold
D^*K	0.03704	0.01852	0	2504
D^*K	0.04630	0.09259	2	2504
$D_s^*\eta$	0.00803	0.00402	0	2660
$D_s^*\eta$	0.01004	0.02009	2	2660
DK^*	0.03704	0.01852	0	2761
DK^*	0.04630	0.09259	2	2761
D^*K^*	0	0.01852	0	2902
D^*K^*	0.01389	0.09259	2	2902
$D_s\phi$	0.01852	0.00926	0	2988
$D_s\phi$	0.02315	0.04630	2	2988
$D_s^*\eta'$	0.01048	0.00524	0	3069
$D_s^*\eta'$	0.01310	0.02621	2	3069
$D_s^*\phi$	0	0.00926	0	3132
$D_s^*\phi$	0.06944	0.04630	2	3132

states. So we restrict ourselves to the open and closed PV and VV channels in the present investigation, but we shall further discuss this issue below. The here included channels for $c\bar{q}$ and $c\bar{s}$ are given in Tables I and II, respectively, together with the corresponding orbital angular momenta, threshold energies, and ground-state couplings squared $(\tilde{g}_{(S=1(0),n=0)}^i)^2$, where $S = 1(0)$ refers to the 3P_1 (1P_1) quark-antiquark component. In Appendix A, we show in more detail how the ground-state coupling constants in Tables I and II depend on the isospin and J^{PC} quantum numbers of the various meson-meson channels. The latter squared couplings, computed in the very general framework of Ref. [16], must be multiplied by $(n+1)/4^n$ for $L = 0$ and by $(2n/5+1)/4^n$ for $L = 2$, so as to obtain the couplings for the radial recurrences n in the RSE sum of Eq. (3). Note that the scheme of Ref. [16] employs overlaps of HO wave functions for the original $q\bar{q}$ pair, the 3P_0 $q\bar{q}$ pair created out of the vacuum, and the outgoing mesons. This allows to rigorously calculate the coupling constants of all excited states as well, in contrast with approaches using combinations of Clebsch-Gordan coefficients only. Nevertheless, our ground-state couplings are identical to the usual ones in practically all situations, including the present one. Finally, a sub-threshold suppression of closed channels is used just as in Ref. [14].

The energies of the bare AV $c\bar{q}$ and $c\bar{s}$ states we determine, as in previous work (see e.g. Refs. [14, 15]), from an HO spectrum. The corresponding constant oscillator frequency and the constituent masses of the charmed, strange, and nonstrange quarks are also kept completely unchanged at the values $\omega = 190$ MeV, $m_c = 1562$ MeV, $m_s = 508$ MeV, and $m_n = 406$ MeV [14, 15]. This yields masses of 2443 MeV and 2545 MeV for the bare AV $c\bar{q}$ and $c\bar{s}$ states, respectively, which are very close to values found in typical single-channel quark models [4, 5].

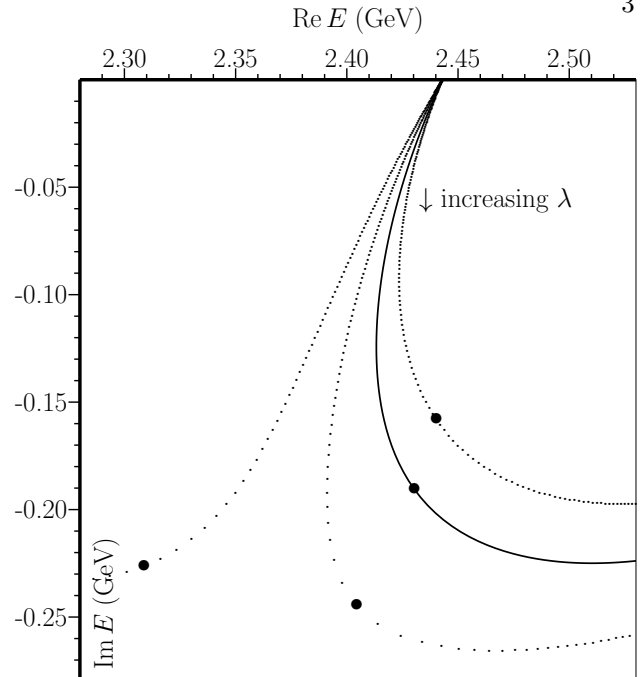


FIG. 1: $D_1(2430)$ pole trajectories as a function of λ , for $r_0 = 3.2\text{--}3.5$ GeV^{-1} (left to right). Solid curve and bullets correspond to $r_0 = 3.40$ GeV^{-1} and $\lambda = 1.30$, respectively.

IV. QUASI-BOUND STATES IN THE CONTINUUM AND OTHER POLES

Next we search for poles in the S matrix. Starting with the $c\bar{q}$ case, we choose r in the range $3.2\text{--}3.5$ GeV^{-1} ($0.64\text{--}0.70$ fm), which is in between the values of 2.0 GeV^{-1} [15] for an AV $c\bar{c}$ system and 4.0 GeV^{-1} [14] for vector $s\bar{s}$ states. In Fig. 1, we plot several pole trajectories in the complex E plane as a function of the overall coupling λ . We see that this pole rapidly acquires a large imaginary part, whereas the real part changes considerably less, especially in the range $r_0 = 3.3\text{--}3.5$ GeV^{-1} , making it a good candidate for the broad $D_1(2430)$ resonance. For $\lambda = 1.30$ and $r_0 = 3.40$ GeV^{-1} , the pole comes out at $(2430 - i \times 191)$ MeV, being thus fine-tuned to the experimental mass and width [1]. However, there should be another pole in the S matrix, since there are 2 quark-antiquark channels and more than 2 MM channels. From the structure of the T matrix in Eqs. (1–3), one can algebraically show that the number of poles for each bare state is equal to $\min(N_{q\bar{q}}, N_{MM})$, besides possible poles of a purely dynamical nature. Indeed, another pole originating from the bare $c\bar{q}$ state is encountered, with its trajectories depicted in Fig. 2. Quite remarkably, this pole moves very little, acquiring an imaginary part that is a factor 55 smaller than in the $D_1(2430)$ case, for the values $\lambda = 1.30$ and $r_0 = 3.40$ GeV^{-1} (see solid lines and bullets in both figures). So this resonance, with a pole position of $(2439 - i \times 3.5)$ MeV, almost decouples from the only open OZIA MM channel [17], viz. $D^*\pi$, representing a quasi-bound state in the continuum (QBSC)

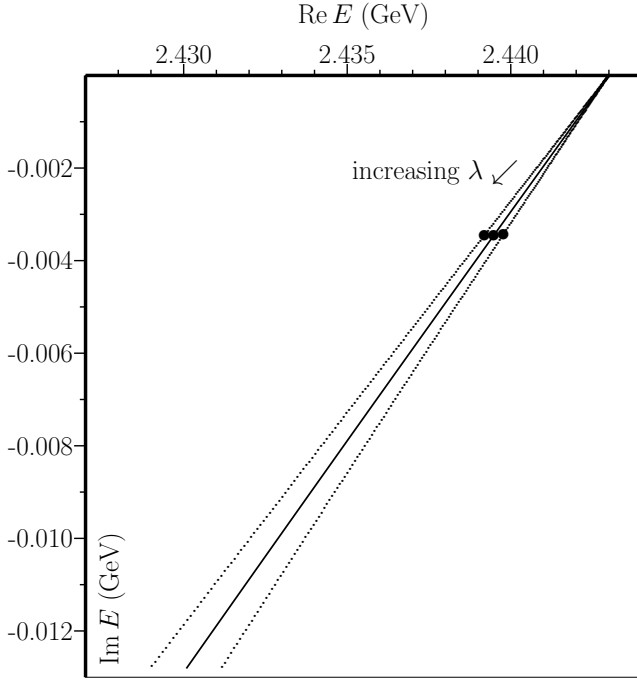


FIG. 2: $D_1(2420)$ pole trajectories as a function of λ , for $r_0 = 3.3\text{--}3.5\text{ GeV}^{-1}$ (left to right). Solid curve and bullets correspond to $r_0 = 3.40\text{ GeV}^{-1}$ and $\lambda = 1.30$, respectively.

[11]. Moreover, it is a good candidate for the $D_1(2420)$, though its width of roughly 7 MeV is somewhat too small and its mass 16 MeV too high. These minor discrepancies may be due to the neglect of the PS channels, with broad resonances in the final states, as suggested above.

Nevertheless, these encouraging results might be partly due to a fortuitous choice of the parameters λ and r_0 . Therefore, we now check the $c\bar{s}$ system, thereby scaling r_0 and λ with the square root of the reduced quark mass (see Ref. [17], Eq. (13)), so as to respect flavor independence of our equations, which yields the $c\bar{s}$ values $r_0 = 3.12\text{ GeV}^{-1}$ and $\lambda = 1.19$. The ensuing $c\bar{s}$ pole trajectories are depicted in Fig. 3, but now for $r_0 = 3.12\text{ GeV}^{-1}$ only. Thus, for $\lambda = 1.19$, the strongly coupling state comes out at 2452 MeV, i.e., only 7.5 MeV below the $D_{s1}(2460)$ mass, with a vanishing width, as the pole ends up below the lowest OZIA channel. As for the $c\bar{s}$ QBSC, it indeed shifts very little from the bare state, settling at $(2540 - i \times 0.7)\text{ MeV}$, i.e., only 5 MeV above the $D_{s1}(2536)$ mass, and having a width fully compatible with experiment [1].

Besides the above ground-state AV charmed mesons, the present model of course also predicts higher recurrences of these resonances. However, due caution is necessary so as to account for the most relevant open and closed decay channels at the relevant energy scales. Now, the first radially excited HO levels of the $^3P_1/1P_1\ c\bar{n}$ and $c\bar{s}$ states lie at 2823 MeV and 2925 MeV, respectively, which allows the corresponding resonances to be reasonably described by the channels included in Tables I,

II. Thus, we find again 4 poles, tabulated in Table III, together with those of the ground-state AV charmed

TABLE III: Poles of ground-state ($n=0$) and first radially-excited ($n=1$) AV charmed mesons. Parameters: $\lambda = 1.30$ (1.19) and $r_0 = 3.40$ (3.12) GeV^{-1} , for $c\bar{q}$ ($c\bar{s}$) states.

Quark Content	Radial Excitation	Pole in MeV
$c\bar{q}$	0	$2439 - i \times 3.5$
$c\bar{q}$	0	$2430 - i \times 191$
$c\bar{s}$	0	$2540 - i \times 0.7$
$c\bar{s}$	0	$2452 - i \times 0.0$
$c\bar{q}$	1	$2814 - i \times 7.8$
$c\bar{q}$	1	$2754 - i \times 47.2$
$c\bar{s}$	1	$2915 - i \times 6.7$
$c\bar{s}$	1	$2862 - i \times 25.7$

mesons. For the radially excited states, we observe a similar pattern as for the ground states, namely two poles that remain close to the bare HO levels, whereas two other poles shift considerably. Note, however, that the difference is not as dramatic as in the $n=0$ case. This may be due to the fact that several decay channels are open now. As for a possible observation of the here predicted $2P_1$ states, no experimental candidates have been reported so far. Namely, in the nearby $c\bar{q}$ mass region, the two listed [1] resonances $D(2600)$ and $D(2750)$ [1] both decay to $D^*\pi$ and $D\pi$, which excludes an AV assignment.

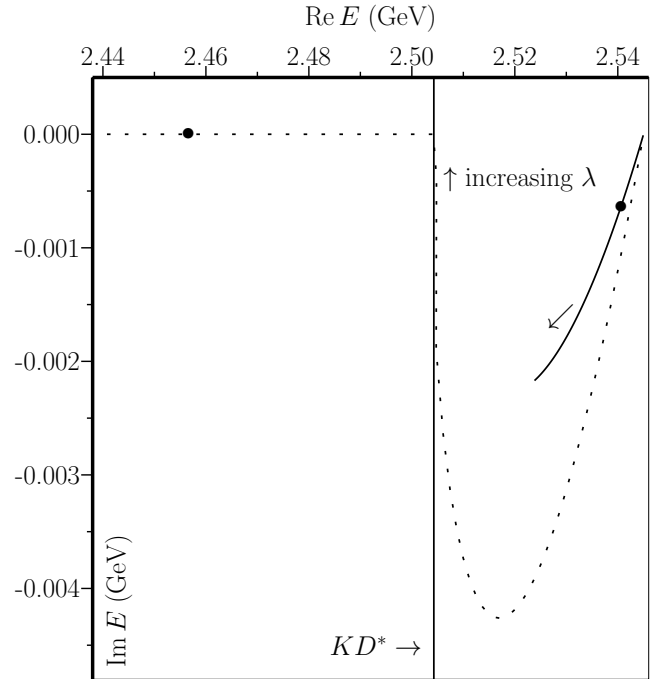


FIG. 3: $D_{s1}(2460)$ (dashed) and $D_{s1}(2536)$ (solid) pole trajectories as a function of λ , for $r_0 = 3.12\text{ GeV}^{-1}$. Bullets correspond to $\lambda = 1.19$; vertical line shows D^*K threshold.

Concerning the $c\bar{s}$ sector, the only listed [1] state around 2.8–2.9 GeV is the $D_{sJ}^*(2860)$ [18], with natural parity and so not an AV, decaying to D^*K and DK , which makes it a good candidate for the 2^3P_2 state, possibly overlapped by the 2^3P_0 [19]. Note that the lower of our two predicted $2P_1$ resonances also practically coincides with the $D_{sJ}^*(2860)$, both in mass and width. This may be a further indication that the $D_{sJ}^*(2860)$ structure corresponds to more than one resonance only.

To conclude this section, we study — for the $c\bar{q}$ system — the dependence of the lowest-lying poles on the number of included quark-antiquark and MM channels. In Table IV, besides the $D_1(2420)$ and $D_1(2430)$ poles

TABLE IV: Poles of AV $c\bar{q}$ mesons, for different sets of included channels. Parameters: $\lambda = 1.30$, $r_0 = 3.40$ GeV $^{-1}$.

$c\bar{q}$ channels	MM channels	Pole 1 (MeV)	Pole 2 (MeV)
$^3P_1 + ^1P_1$	20	$2430 - i \times 191$	$2439 - i \times 3$
$^3P_1 + ^1P_1$	2	$2402 - i \times 36$	$2441 - i \times 1$
$^3P_1 + ^1P_1$	1	$2431 - i \times 39$	-
3P_1	20	$2409 - i \times 65$	-
1P_1	20	$2425 - i \times 96$	-

resulting from the full calculation, with the 20 MM channels from Table I, we first give the pole positions for the cases that only 2 ($D^*\pi$, $L = 0, 2$) or 1 ($D^*\pi$, $L = 0$) MM channels are included. The last two poles then correspond to calculations with the full 20 MM channels but only one quark-antiquark channel, viz. 3P_1 or 1P_1 . Notice that only one pole is found when the number of quark-antiquark or MM channels is equal to 1. This confirms our above conjecture that the number of poles for each bare HO level is given by $\min(N_{q\bar{q}}, N_{MM})$.

V. SUMMARY AND CONCLUSIONS

In the foregoing, we have managed to rather accurately reproduce the masses and widths of the $D_1(2420)$, $D_1(2430)$, $D_{s1}(2536)$, and $D_{s1}(2460)$ with only 2 free parameters, one of which is already constrained by previous model calculations, as well as by reasonable estimates for the size of these mesons. Crucial is the approximate decoupling from the continuum of one combination of 3P_1 and 1P_1 components, which amounts to a mixing angle close to 35° . Namely, if we express a QBSC as $|\text{QBSC}\rangle = -\sin\theta|{}^3P_1\rangle + \cos\theta|{}^1P_1\rangle$, it decouples from the $L=0$ $D^*\pi$ channel (for $c\bar{q}$) or D^*K channel (for $c\bar{s}$), if $\theta = \arccos\sqrt{2/3} \approx 35.26^\circ$ (see Tables I, II). Inclusion of the other, practically all closed, channels apparently changes the picture only slightly in our formalism. This result is in full agreement with the findings in Ref. [12]. However, in the present approach this particular mixing [20] comes out as a completely dynamical result, and is not chosen by us beforehand. Moreover, the bare-mass degeneracy of 3P_1 and 1P_1 states is adequately lifted via

the decay couplings in Tables I and II, dispensing with the usual $\vec{S} \cdot \vec{L}$ splitting. Also note that the occurrence of (approximate) bound states in the continuum for AV charmed mesons had already been conjectured by two of us [17], based on more general arguments.

The puzzling discrepancy between the AV-V mass splittings in the $c\bar{q}$ and $c\bar{s}$ sectors is resolved in our calculation by dynamical, nonperturbative coupled-channel effects. A similar phenomenon we have observed before [21] for the $D_0^*(2300\text{--}2400)$ [1] resonance, and may be related to an effective Adler-type zero [22] in the $D^*\pi$ and $D\pi$ channels in the AV and scalar $c\bar{n}$ cases, respectively, owing to the small pion mass.

Summarizing, we have reproduced the whole pattern of masses and widths of the AV charmed mesons dynamically, by coupling the most important open and closed two-meson channels to bare $c\bar{q}$ and $c\bar{s}$ states containing both 3P_1 and 1P_1 components. The dynamics of the coupled-channel equations straightforwardly leads to one pair of strongly shifted states and another pair of QBSCs. Ironically, the state that shifts most in mass, namely the $D_{s1}(2460)$, ends up as the narrowest resonance. This emphasizes the necessity [23] to deal with unquenched meson spectroscopy in a fully nonperturbative framework.

One might argue that these conclusions will depend on the specific model employed. Admittedly, our numerical results could change somewhat if slightly different bare masses for the AV charmed mesons were chosen, non- S -wave decay channels were included as well, or a different scheme was used to calculate the decreasing couplings of the higher recurrences. Nevertheless, we are convinced the bulk of our results will not change, most notably the appearance of QBSCs and the large shifts of their partner states, as the almost inevitable consequence of exact nonperturbative coupled-channel dynamics.

Acknowledgments

This work was supported in part by the *Fundação para a Ciência e a Tecnologia* of the *Ministério da Ciência, Tecnologia e Ensino Superior* of Portugal, under contract CERN/FP/116333/2010 and grant SFA-2-91/CFIF.

Appendix A: Three-meson couplings

The ground-state couplings in Tables I and II are obtained by multiplying the isospin recouplings given in Table V with the J^{PC} couplings in Table VI, for an OZIA process $M_A \rightarrow M_B + M_C$ based on 3P_0 $q\bar{q}$ creation [16]. For clarity, we represent here all couplings by rational numbers. Note that η_n and η_s in Table V stand for the pseudoscalar $I = 0$ states $(u\bar{u} + d\bar{d})/\sqrt{2}$ and $s\bar{s}$, respectively. Then, we get the couplings to the physical η and η' mesons by applying a mixing angle — in the flavor basis — of 41.2° , as in Ref. [21], 2nd paper. For the ω and ϕ we assume ideal mixing.

TABLE V: Squared isospin recouplings for the 3-meson process $M_A \rightarrow M_B + M_C$, with $M_A = c\bar{s}$ or $c\bar{q}$.

M_A	M_B	M_C	g_I^2
D_{s1}	D_s, D_s^*	η_s, ϕ	1/3
D_{s1}	D, D^*	K, K^*	2/3
D_1	D_s, D_s^*	K, K^*	1/3
D_1	D, D^*	π, ρ	1/2
D_1	D, D^*	η_n, ω	1/6

TABLE VI: Squared ground-state coupling constants for the 3-meson process $M_A \rightarrow M_B + M_C$, with $J^{PC}(M_A) = 1^{+\pm}$, and M_A, M_B belonging to the lowest pseudoscalar or vector nonet.

$J^{PC}(M_A)$	$J^{PC}(M_B)$	$J^{PC}(M_C)$	$L_{M_B M_C}$	$S_{M_B M_C}$	$g_{(n=0)}^2$
1^{++}	0^{-+}	1^{--}	0	1	1/18
1^{++}	0^{-+}	1^{--}	2	1	5/72
1^{++}	1^{--}	1^{--}	0	1	0
1^{++}	1^{--}	1^{--}	2	2	5/24
1^{+-}	0^{-+}	1^{--}	0	1	1/36
1^{+-}	0^{-+}	1^{--}	2	1	5/36
1^{+-}	1^{--}	1^{--}	0	1	1/36
1^{+-}	1^{--}	1^{--}	2	1	5/36

-
- [1] K. Nakamura *et al.* [Particle Data Group], J. Phys. G **37**, 075021 (2010).
- [2] D. Besson *et al.* [CLEO Collaboration], Phys. Rev. D **68**, 032002 (2003) [Erratum-ibid. D **75**, 119908 (2007)].
- [3] K. Abe *et al.* [Belle Collaboration], Phys. Rev. D **69**, 112002 (2004).
- [4] S. Godfrey and N. Isgur, Phys. Rev. D **32**, 189 (1985).
- [5] M. Di Pierro and E. Eichten, Phys. Rev. D **64**, 114004 (2001).
- [6] W. A. Bardeen, E. J. Eichten, and C. T. Hill, Phys. Rev. D **68**, 054024 (2003).
- [7] D. Becirevic, S. Fajfer, and S. Prelovsek, Phys. Lett. B **599**, 55 (2004).
- [8] P. Colangelo, F. De Fazio, and R. Ferrandes, Mod. Phys. Lett. A **19**, 2083 (2004).
- [9] T. Mehen and R. P. Springer, Phys. Rev. D **72**, 034006 (2005).
- [10] D. Gamermann and E. Oset, Eur. Phys. J. A **33**, 119 (2007).
- [11] F. K. Guo, P. N. Shen, and H. C. Chiang, Phys. Lett. B **647**, 133 (2007).
- [12] A. M. Badalian, Yu. A. Simonov, and M. A. Trusov, Phys. Rev. D **77**, 074017 (2008).
- [13] E. van Beveren and G. Rupp, Annals Phys. **324**, 1620 (2009).
- [14] S. Coito, G. Rupp, and E. van Beveren, Phys. Rev. D **80**, 094011 (2009).
- [15] S. Coito, G. Rupp, and E. van Beveren, Eur. Phys. J. C **71**, 1762 (2011).
- [16] E. van Beveren, Z. Phys. C **21**, 291 (1984).
- [17] E. van Beveren and G. Rupp, Eur. Phys. J. C **32**, 493 (2004).
- [18] B. Aubert *et al.* [BABAR Collaboration], Phys. Rev. D **80**, 092003 (2009).
- [19] E. van Beveren and G. Rupp, Phys. Rev. D **81**, 118101 (2010).
- [20] Z. Y. Zhou and Z. Xiao, arXiv:1105.6025 [hep-ph].
- [21] E. van Beveren and G. Rupp, Phys. Rev. Lett. **91**, 012003 (2003); **97**, 202001 (2006).
- [22] D. V. Bugg, Phys. Rept. **397**, 257 (2004); G. Rupp, F. Kleefeld, and E. van Beveren, AIP Conf. Proc. **756**, 360 (2005).
- [23] K. P. Khemchandani, E. van Beveren, and G. Rupp, Prog. Theor. Phys. **125**, 581 (2011).